Polyhedron 181 (2020) 114460

Contents lists available at ScienceDirect

Polyhedron

journal homepage: www.elsevier.com/locate/poly

Unrealized concepts of masked alkylidenes in (PNP)FeXY systems and alternative approaches to $L_nX_mFe(IV)$=CHR

Gregory M. George [a], Peter T. Wolczanski [a,*], Samantha N. MacMillan [a], Thomas R. Cundari [b]

[a] Department of Chemistry & Chemical Biology, Baker Laboratory, Cornell University, Ithaca, NY 14853, USA
[b] Department of Chemistry, CASCaM, University of North Texas, Denton, TX 76201, USA

ARTICLE INFO

Article history:
Received 4 December 2019
Accepted 17 February 2020
Available online 21 February 2020

Dedicated to Prof. John E. Bercaw, for teaching us how to be, and enjoy being, scientists.

Keywords:
Iron
Phosphine
Zwitterion
Masking
Alkylidene

ABSTRACT

Treatment of PNP ligands with iron(II) halides yielded pseudo tetrahedral {$(Ph_2PCH_2)_2NR$}FeX_2 (R″ = ^{t}Bu, **1a**-X; Me, **1b**-X) and {$(^iBu_2PCH_2)_2NR''$}FeX_2 (R″ = ^{t}Bu, **2a**-X; Me, **2b**-X) complexes, which could be mono- and dialkylated to afford various {$(Ph_2PCH_2)_2NR''$}FeCl(R) (R″ = ^{t}Bu, **3a**-R; Me, **3b**-R), {$(^iBu_2PCH_2)_2NR''$}FeCl (R) (R″ = ^{t}Bu, **4a**-R; Me, **4b**-R), {$(Ph_2PCH_2)_2N^tBu$}Fe(^{neo}Pe)$_2$ (**5a**-^{neo}Pe) and {$(^iBu_2PCH_2)_2N^tBu$}Fe(1-nor)$_2$ (**6a**-nor). All of the complexes were high spin (S = 2), and structural studies of {$(Ph_2PCH_2)_2NMe$}$FeCl_2$ (**1b**-Cl), {$(^iBu_2PCH_2)_2N^tBu$}$FeCl_2$ (**2a**-Cl), and {$(^iBu_2PCH_2)_2N^tBu$}FeCl(1-nor) (**4a**-nor), revealed chair conformations for the PNP ligands, which were calculated to have modest barriers to boat configurations via twist-boats as calculational minima. Attempts to convert these complexes to zwitterionic NCRR′Fe-containing species as "masked alkylidenes" failed to materialize. Alternative approaches involving structurally characterized diamagnetic {$(^iBu_2PCH_2)_2N^tBu$}$(CO)_2$FeCl(CO^{neo}Pe) (**8**), the carbonylation product of **4a**-^{neo}Pe, and low-valent {$(Ph_2PCH_2CH_2)_2N^tBu$}Fe($(H_2C{=}CHSiMe_2)_2O$) (**9**) also failed. An analysis of orbital energies and overlap is given for alkylidenes. Covalence is identified as a crucial feature necessary for the alkylidene to metalacyclobutane transformation in metathesis.

1. Introduction

The application of transition metals to catalytic olefin metathesis (OM) is practically limited to a select group of metals, most of which are members of the second row [1–5]. While molybdenum is relatively inexpensive and diverse in usage [1,2], ruthenium catalysts are still the leading choice for most fine-chemicals synthesis due to their lesser sensitivity, and relative ease of handling and preparation [3,4]. Somewhat surprisingly, neither first row transition metal alternative – chromium in group 6 [6,7] or iron [8–22] in group 8 – has been shown to exhibit similar 2 + 2, i.e. M=CRR′ + olefin, chemistry, whereas vanadium alkylidenes [23–25] complement metathesis reactivity observed initially from niobium and tantalum [26], and titanium alkylidenes have shown modest catalysis [27–29].

According to theoretical work by Hoffmann, d^n ($n \leq 4$) complexes are a requirement for metathesis activity [30]. Early work on $[CpL_2Fe{=}CRR']^+$ and CpLXFe=CRR′ complexes [8–10,15–17], including a structural characterization of [Cp(dppe)Fe=CHMe]$^+$ [10], afforded examples of cyclopropanation, but no evidence of 2 + 2 chemistry. Subsequent exploration of diaryl carbenes of Fe (IV) also failed to manifest reactivity other than some cyclopropanation [11–14,31], and it is likely that such functionality is better described as diarylcarbyl radicals antiferromagnetically coupled to Fe(III) centers, i.e., $L_nX_mFe^{\uparrow}$(III)(-$C^{\downarrow}Ar_2$) [14,32].

Work in these laboratories initially focused on generating pseudo octahedral Fe(IV) alkylidenes using synthetic approaches derived from Cp-based iron(IV) cation preparation. Three cationic Fe(IV) chelates [20] and eight neutral Fe(IV) derivatives [21], including five structurally characterized examples, were prepared, yet none elicited reactivity that implicated metathesis. In addition, calculations strongly indicated that Fe(IV) cationic alkylidenes can be construed as Fe(II) stabilized carbocations, and the neutrals as highly delocalized Fe(II) species [22]. Consequently, lower coordinate derivatives akin to Grubbs' type catalysts were sought, but while Fe(IV) imido complexes, (IPr)Fe(=NAd)R_2 (R = ^{neo}Pe, 1-nor; Ad = adamantyl) were synthesized [33], corresponding alkylidenes could not be prepared, as shown in Scheme 1, even with a steric mimic of AdN_3, the aziridine Ad-$^cCN_2$ [34].

It is possible that Fe(IV)=CRR′ functionalities are not stable enough in these coordination environments, or that the covalency in the iron-carbon double bond needed for metathesis cannot be obtained, as the alkylidene fragment is simply not oxidizing enough. Since there is modest calculational support for the former, approaches toward masking alkylidenes or carbenes, first

* Corresponding author.
E-mail addresses: ptw2@cornell.edu (P.T. Wolczanski), t@unt.edu (T.R. Cundari).

https://doi.org/10.1016/j.poly.2020.114460
0277-5387/

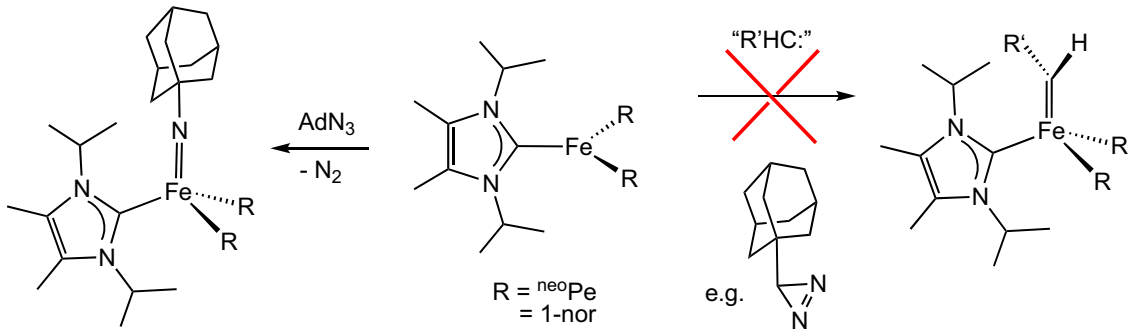

Scheme 1. Synthesis of (IPr)Fe(=NAd)R_2 (R = ^{neo}Pe, 1-nor) and failure to prepare an analogous alkylidene.

exemplified in chemistry from the Deng group [32], were sought. In this chemistry, abbreviated in Scheme 2, di-tolyl- diazomethane was utilized as the carbene source. The resulting cyclpropanations were rationalized via labeling studies on *syn*-α-deuterio styrene cyclopropanation, Hammett substituent studies, and calculations as having substantial radical character in a transient $(PN_2)Fe^{\uparrow}(III)(-C^{\downarrow}Ar_2)$. intermediate. Since previous diarylcarbene Fe(IV) complexes were known to possess radical character [14], perhaps an increase in the field strength at iron might allow "masked alkylidenes" to function in a metathesis capability. As a consequence, we envisage utilizing known $(R'_2PCH_2)_2NR$" ligands as initial chelates, as shown in Fig. 1.

Precedented P,N,P-type ligands containing diisobutyl and diphenyl phosphine units were considered for appraisal [35–40], and standard dihalides, $\{(R'_2PCH_2)_2NR''\}FeX_2$, were targeted, noting that subsequent alkylation would provide an additional means of increasing the field strength of the iron core in order to increase covalency. Three means to introduce the zwitterionic masked alkylidene functionality were considered, as illustrated in Scheme 3. The tetrahedral complexes could be subject to direct alkylidene sources, such as conventional diazo compounds, R_2CN_2 [41,42], with displacement of N_2 by the internal NR″ group serving to mask the R_2C unit and create the zwitterion. Alkylation of the zwitterion should render a tetraalkylammonium cation, and heterolytic CH bond activation, perhaps triggered by an additional base, should render the desired zwitterion. Finally, tetraalkylammonium formation with a dihaloalkane, such as CH_2I_2, would allow a subsequent reductive coupling to introduce the zwitterion.

2. Results and discussion

2.1. $\{(R'_2PCH_2)_2NR''\}FeXY$

2.1.1. $\{(R'_2PCH_2)_2NR''\}FeX_2$ syntheses

The addition of FeX_2 (X = Cl, Br) and $(R'_2PCH_2)_2NR''$(R′ = Ph, R″ = ^{t}Bu, Me) in THF for 16 h in THF at 23 °C afforded $\{(Ph_2PCH_2)_2NR''\}FeX_2$ (R″ = ^{t}Bu, X = Cl (86%), **1a**-Cl; X = Br (85%), **1a**-Br; R″ = Me, X = Cl (87%), **1b**-Cl) in very good yields, affording pale-yellow microcrystalline solids (Scheme 4). The related reaction of $FeCl_2$ and $(R'_2PCH_2)_2NR''$(R′ = ^{i}Bu, R″ = ^{t}Bu, Me) also resulted in $\{(^iBu_2PCH_2)_2NR''\}FeX_2$ (R″ = ^{t}Bu, X = Cl (89%), **2a**-Cl; R″ = Me, X = Cl (87%), **2b**-Cl) as similarly colored solids. All pseudo tetrahedral complexes were high spin ($S = 2$) according to Evans' method measurements [43]: **1a**-Cl, 5.6 μ_B; **1a**-Br, 5.5 μ_B; **1b**-Cl, 5.2 μ_B; **2a**-Cl, 5.0 μ_B; **2b**-Cl, 5.6 μ_B).

2.1.2. Molecular structure of $\{(Ph_2PCH_2)_2NMe\}FeCl_2$ (**1b**-Cl)

The molecular view of $\{(Ph_2PCH_2)_2NMe\}FeCl_2$ (**1b**-Cl) in Fig. 2 reveals a pseudo tetrahedral structure with the PNP ligand in a chair configuration with an equatorial NMe substituent and the lone pair axial. In this geometry, any modest Me/Ph interaction is minimized, and the Fe-Cl2 bond is ~ 90° to the NMe. The core angle and distances are given in the caption of Fig. 2 and all distances are consistent with a high spin iron center, with $d(FeP)_{ave}$ = 2.422(10) Å and $d(FeCl)_{ave}$ = 2.228(14) Å. The bite angle of the PNP ligand is 90.024(15)°, causing some variation away from a regular tetrahedron, with ∠Cl1-Fe-Cl2 = 125.73(2)°, and the Cl-Fe-P angles varying from 99.977(17) – 118.454(19)°, with the angles to Cl1 wider than those to Cl2, presumably due to the influence of the two adjacent axial phenyl substituents.

2.1.3. Molecular structure of $\{(^iBu_2PCH_2)_2N^tBu\}FeCl_2$ **2a**-Cl)

Fig. 3 illustrates a molecular view of $\{(^iBu_2PCH_2)_2N^tBu\}FeCl_2$ **2a**-Cl), and the diisobutylphosphine variant deviates little from **1b**-Cl. The bite angle of the PNP ligand is slightly wider at 92.405(13)°, and its configuration is again a chair, with the ^{t}Bu group in an equatorial position, again roughly 90° with respect to the FeCl2 bond. The caption of Fig. 3 provides the remaining core distances and angles, and any subtle variation can be rationalized on the basis of slightly increased sterics among the isobutyl groups. As Fig. 3 reveals, the chair is quite regular except for subtle variation in the equatorial 2-propyl groups.

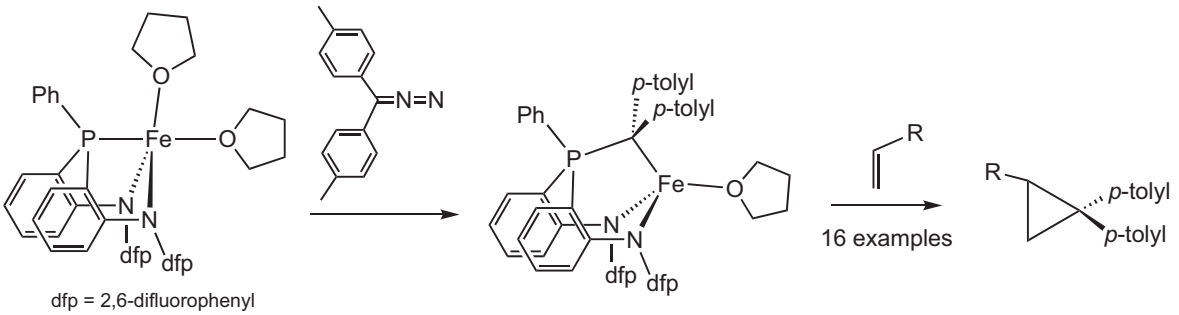

Scheme 2. Cyclopropanation via Deng's "masked" di-tolyl-carbene complex.

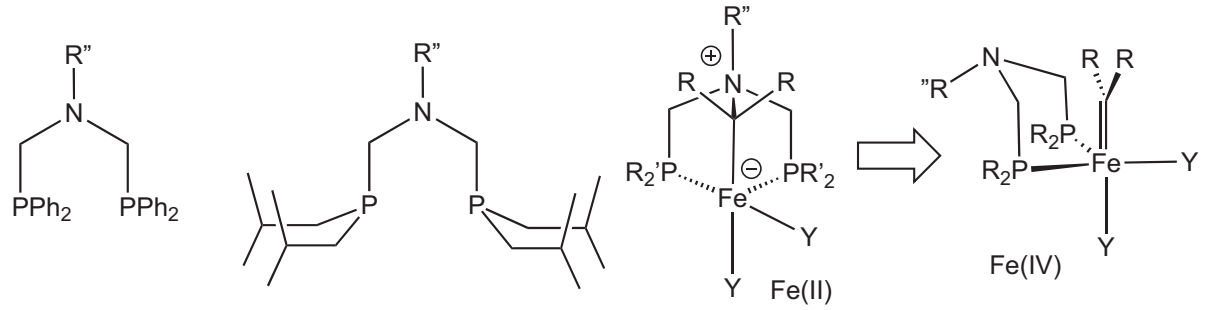

Fig. 1. Featured ligands toward potential masked alkylidenes.

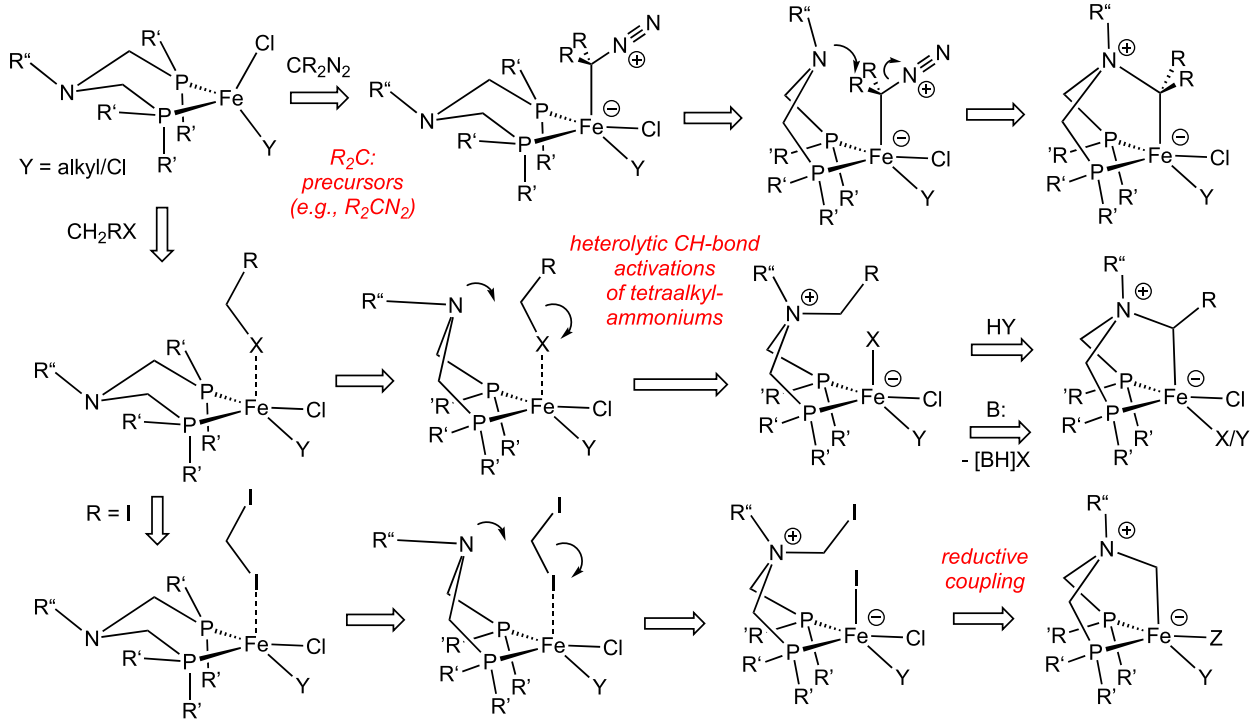

Scheme 3. Three approaches to zwitterionic masked alkylidenes: 1) alkylidene precursors; 2) heterolytic CH-bond activation; and 3) reductive coupling.

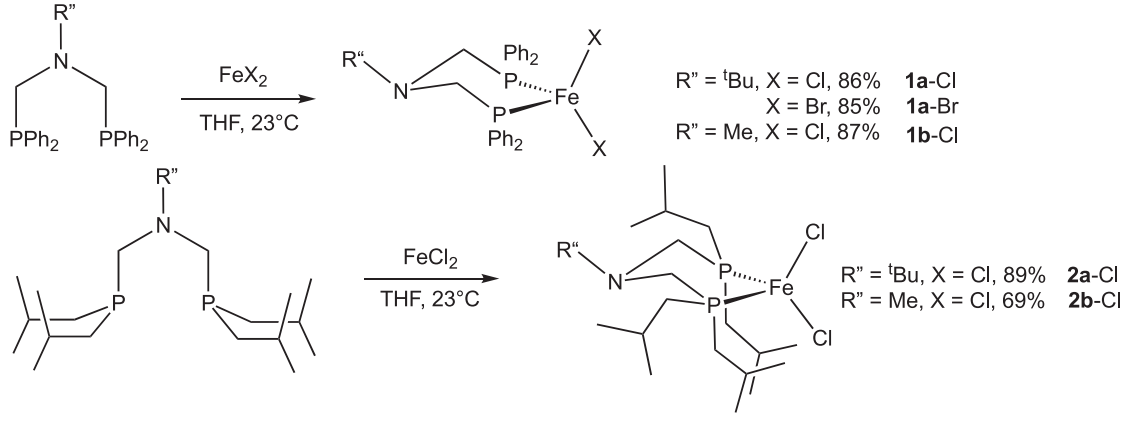

Scheme 4. Di(phosphinomethyl)alkylamine iron dihalide syntheses.

2.1.4. {(R′2PCH2)2NR″}FeXR syntheses

The dichlorides were chosen as substrates for alkylation with RLi (R = 1-nor, ^{neo}Pe, CH_2SiMe_3), and the reactions are illustrated in Scheme 5. The bulkier alkyllithiums were chosen to lessen the probability of aggregation difficulties, and treatment of {(Ph_2PCH_2)$_2$NR″}$FeCl_2$ (R″ = ^{t}Bu, **1a**-Cl; Me, **1b**-Cl) generated

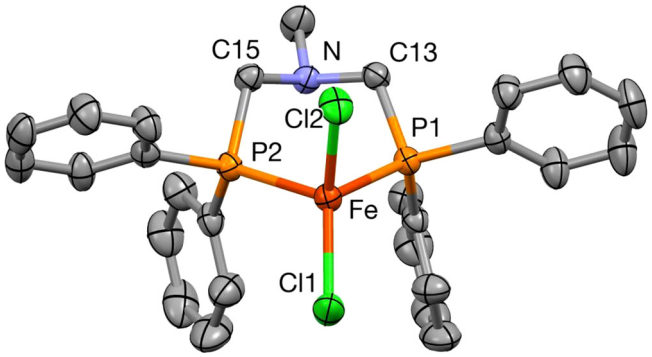

Fig. 2. Molecular view of {($Ph_2PCH_2)_2$NMe}$FeCl_2$ (**1b**-Cl); ellipsoids at 50%. Core interatomic distances (Å) and angles (°): FeCl1, 2.2180(5); FeCl2, 2.2380(5); FeP1, 2.4285(4); FeP2, 2.4144(4); Cl1-Fe-Cl2, 125.73(2); Cl1-Fe-P1, 118.454(19); Cl1-Fe-P2, 113.632(19); Cl2-Fe-P1, 99.977(17); Cl2-Fe-P2, 102.332(18); P1-Fe-P2, 90.024(15).

{($Ph_2PCH_2)_2$NR″}FeCl(R) (R″ = ^{t}Bu, R = 1-nor, **3a**-nor, 75%, ^{neo}Pe, **3a**-^{neo}Pe, 70%, CH_2SiMe_3, **3a**-CH_2SiMe_3, 87%; R″ = Me, R = 1-nor, **3**b-nor, 45%, CH_2SiMe_3, **3**b-CH_2SiMe_3, 46%). Likewise, the addition of RLi to {(^{i}Bu$_2$PCH$_2$)$_2$NR″}$FeCl_2$ (R″ = ^{t}Bu, **2a**-Cl; R″ = Me, **2b**-Cl) afforded {(^{i}Bu$_2$PCH$_2$)$_2$NR″}FeCl(R) (R″ = ^{t}Bu, R = 1-nor, **4a**-nor, 59%, ^{neo}Pe, **4a**-^{neo}Pe, 57%, CH_2SiMe_3, **4a**-CH_2SiMe_3, 82%; R″ = Me, R = 1-nor, **4b**-nor, CH_2SiMe_3, **4b**-CH_2SiMe_3, 63%). All alkylations proceeded in modest yields, and while most produced yellow containing microcrystalline samples, not all reactions were clean. For example, a yield of pure **4b**-nor could not be obtained, and in virtually every alkylation, some Fe(1-nor)$_4$ (typically ~5%) was produced [44], indicative of some disproportionation. Alkylation did not appreciably increase the field strength of the pseudo tetrahedral derivatives, as Evans' method measurements [43] were consistent with S = 2 iron centers: **3a**-nor, μ = 5.1 μ_B, **3a**-^{neo}Pe, μ = 5.6 μ_B, **3a**-CH_2SiMe_3, μ = 5.2 μ_B, **3b**-nor, μ = 5.3 μ_B, **3b**-CH_2SiMe_3, μ = 5.6 μ_B, **4a**-nor, μ = 4.7 μ_B, **4a**-^{neo}Pe, μ = 4.8 μ_B, **4a**-CH_2SiMe_3, μ = 5.4 μ_B, **4b**-nor, μ = 5.1 μ_B, **4b**-CH_2SiMe_3, μ = 5.1 μ_B.

2.1.5. Molecular structure of {($Ph_2PCH_2)_2$NMe}FeCl(1-nor) (**4a**-nor)

As in the cases of **1b**-Cl and **2a**-Cl, Fig. 4 indicates a pseudo tetrahedral structure with near mirror symmetry. Its caption lists the core metric values, and these are also similar, except that the 1-norbornyl ligand exerts modest steric influence. The PNP bite angle is slightly reduced to 88.684(12)°, the Cl-Fe-P angles average 100.8(37)°, the C23-Fe-P angles are 122.7(29)° (ave) and the C23-Fe-Cl angle is only 115.86(4)°. The Fe-P and Fe-Cl distances are essentially the same, and the unique d(Fe-C23) = 2.0509(13) Å, as expected for high spin tetrahedral iron.

2.1.6. {($R'_2PCH_2)_2$NR″}FeR_2 syntheses

Dialkylations were also conducted with {($Ph_2PCH_2)_2$NR″}$FeCl_2$ (R″ = ^{t}Bu, **1a**-Cl; Me, **1b**-Cl) and {(^{i}Bu$_2$PCH$_2$)$_2$NR″}$FeCl_2$ (R″ = ^{t}Bu, **2a**-Cl; R″ = Me, **2b**-Cl), but here the isolation of clean products, as shown in Scheme 6, were limited to {($Ph_2PCH_2)_2$N^{t}Bu}Fe(^{neo}Pe)$_2$ (**5a**-^{neo}Pe, 50%, μ = 5.3 μ_B) and {(^{i}Bu$_2$PCH$_2$)$_2$N^{t}Bu}Fe(1-nor)$_2$ (**6a**-nor, 58%), μ = 5.5 μ_B). At this point, further exploration, purification and isolation of alkyl and dialkyl derivatives was halted because this approach to masked alkylidenes appeared fruitless (*vide infra*).

2.2. Attempts at masked alkylidenes

With several PNP-dihalides, alkyl-halides, and dialkyls in hand, the approaches proffered in Scheme 3 were attempted. Without elaboration, common diazo-species failed to deliver alkylidene fragments, including every variant with Ph_2CN_2, and decomposition was common (Scheme 7). *N*-alkylation attempts were made with a variety of RX and CH_2I_2, and surprisingly, no *N*-alkylation was observed, even with the far less crowded *N*-Me ligands, and even under elevated temperatures that eventually led to decomposition. With certain highly reactive reagents, such as *p*-$MeOC_6H_4$-CH_2Br, phosphine alkylation was determined to occur upon degradation.

2.3. Conformational studies

The lack of alkylation success prompted consideration of a steric or conformational bias, and DFT calculations [45–47] were brought to bear on the latter, with {($Ph_2PCH_2)_2$N^{t}Bu}$FeCl_2$ (**1b**-Cl) {($Ph_2PCH_2)_2$NMe}$FeCl_2$ (**1b**-Cl) the subjects of the study in Fig. 5. While the transition state ascribed to the chair to boat conformational change was only ~9.7 kcal/mol, the latter was not a stable configuration, and twist-boat conformers were found to be stable instead, at 3.7 kcal/mol relative to the chair. Since the interconversions are relatively facile, there would appear to be no significant impediment to alkylation. However, if the iron center acts as a Lewis acid as expected, the orientation of the *N*-lone pair could

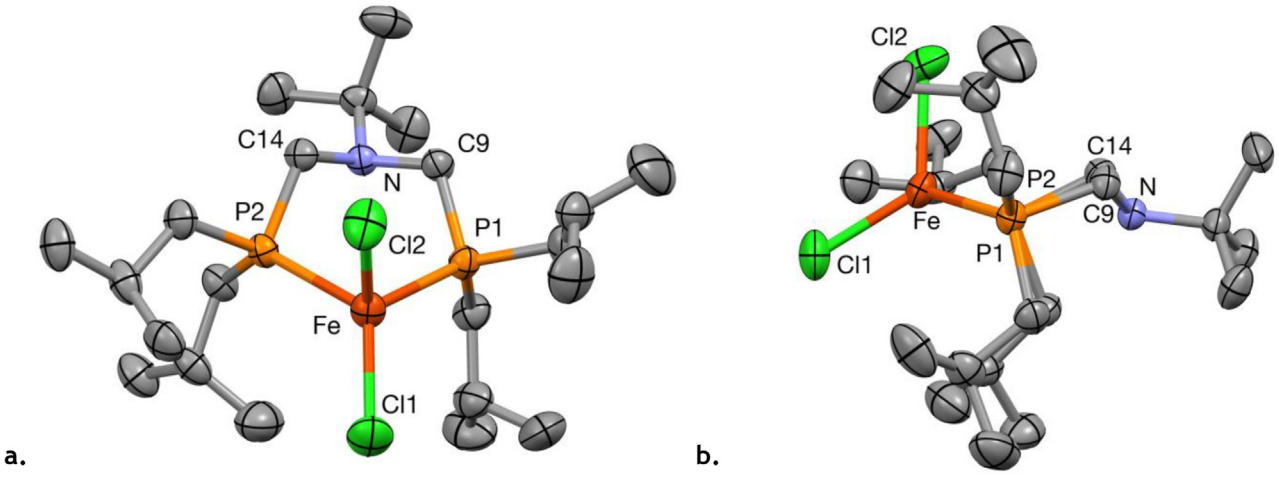

Fig. 3. Molecular view of {(^{i}Bu$_2$PCH$_2$)$_2$N^{t}Bu}$FeCl_2$ (**2a**-Cl, **a.**) and another with phosphines eclipsed (**b.**); ellipsoids at 50%. Core interatomic distances (Å) and angles (°): FeCl1, 2.2271(5); FeCl2, 2.2553(5); FeP1, 2.4289(4); FeP2, 2.4459(4); Cl1-Fe-Cl2, 123.29(2); Cl1-Fe-P1, 114.414(17); Cl1-Fe-P2, 119.947(17); Cl2-Fe-P1, 106.091(17); Cl2-Fe-P2, 95.180(16); P1-Fe-P2, 92.405(13).

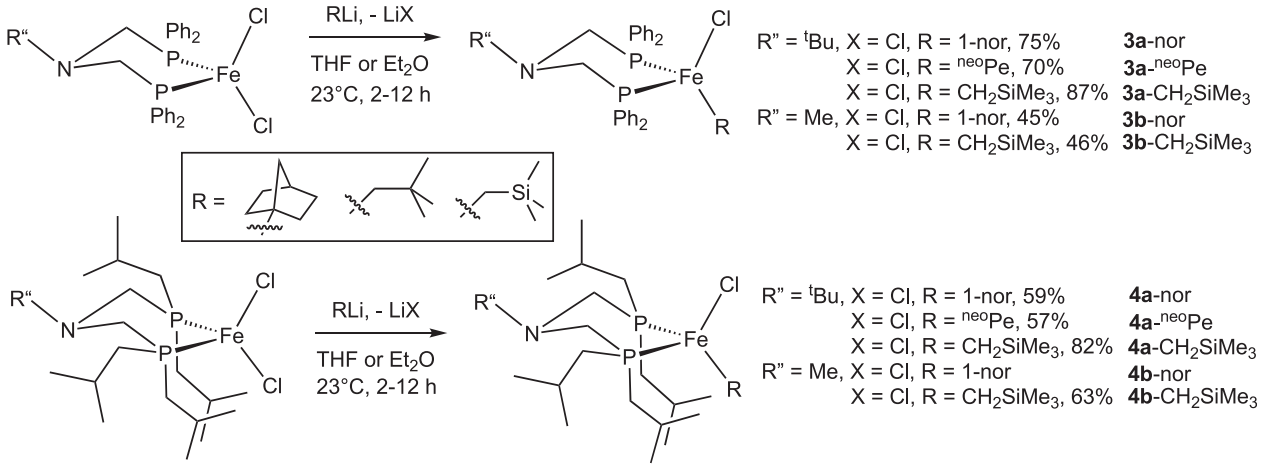

Scheme 5. Alkylations of $\{(R'_2PCH_2)_2NR''\}FeX_2$ with RLi (R = 1-nor, ^{neo}Pe, CH_2SiMe_3).

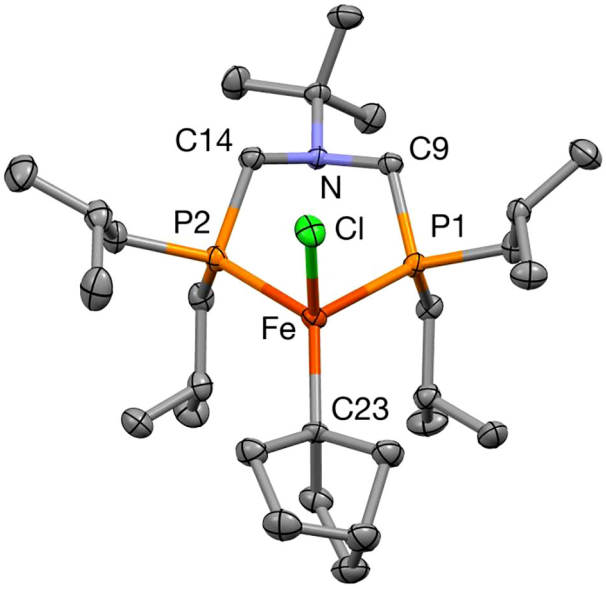

Fig. 4. Molecular view of $\{(^iBu_2PCH_2)_2N^tBu\}FeCl$(1-nor) (**4a**-nor); ellipsoids at 50%. Core interatomic distances (Å) and angles (°): FeCl, 2.2840(4); FeC23, 2.0509(13); FeP1, 2.4649(3); FeP2, 2.4439(4); Cl1-Fe-C23, 115.86(4); Cl1-Fe-P1, 103.399(13); Cl1-Fe-P2, 98.207(13); C23-Fe-P1, 120.60(4); C23-Fe-P2, 124.74(4); P1-Fe-P2, 88.684(12).

be critical to alkylation, and entropic factors leading to the proper TS for attack at RX···Fe might be prohibitive since the complexes are not that thermally stable.

2.4. Syntheses of $\{(Ph_2PCH_2CH_2)_2N^tBu\}FeXY$ and RX addition

With the possibility of conformational difficulties present, a floppier PNP ligand was employed, and Scheme 8 reveals the syntheses of $\{(Ph_2PCH_2CH_2)_2N^tBu\}FeCl_2$ (**7**-Cl) [48] and $\{(Ph_2PCH_2CH_2)_2N^tBu\}FeCl$(1-nor) (**7**-nor). Unfortunately, while the dichloride was isolated cleanly (61%), the norbornyl-chloride was prepared in low yield, as substantial quantities of $(1\text{-nor})_4Fe$ [44] were again produced as a byproduct. Nonetheless alkylation attempts with the complexes were made without success, and once again the highly reactive *p*-$MeOC_6H_4CH_2Br$ appeared to alkylate at phosphorus.

2.5. Carbonylation of **4a**-^{neo}Pe to $\{(^iBu_2PCH_2)_2N^tBu\}(CO)_2FeCl$ ($CO^{neo}Pe$) (**8**)

Failure to achieve masking of alkylidenes via the routes exhibited in Scheme 3 prompted consideration of elaboration of Fischer carbene species, as shown in Scheme 9. Carbonylation of $\{(^iBu_2PCH_2)_2N^tBu\}FeCl(^{neo}Pe)$ (**4a**-^{neo}Pe) was explored as an entry into a masked Fischer carbene. As as eq 1 reveals, carbonylation could not be restricted to one CO, although acyl formation was noted. Two terminal stretching frequencies at 2009 and 1954 cm^{-1}, and

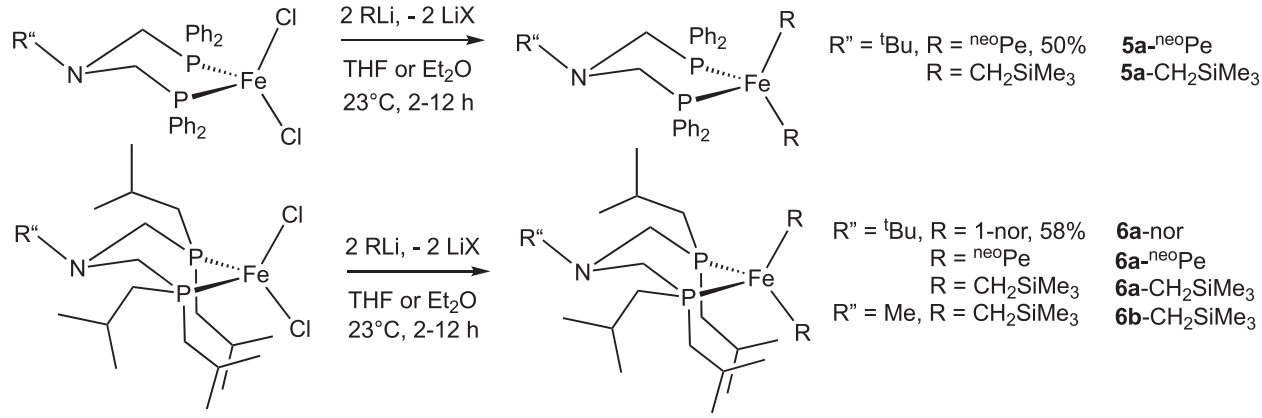

Scheme 6. Dialkylations of $\{(R'_2PCH_2)_2NR''\}FeX_2$ with RLi (R = 1-nor, ^{neo}Pe, CH_2SiMe_3).

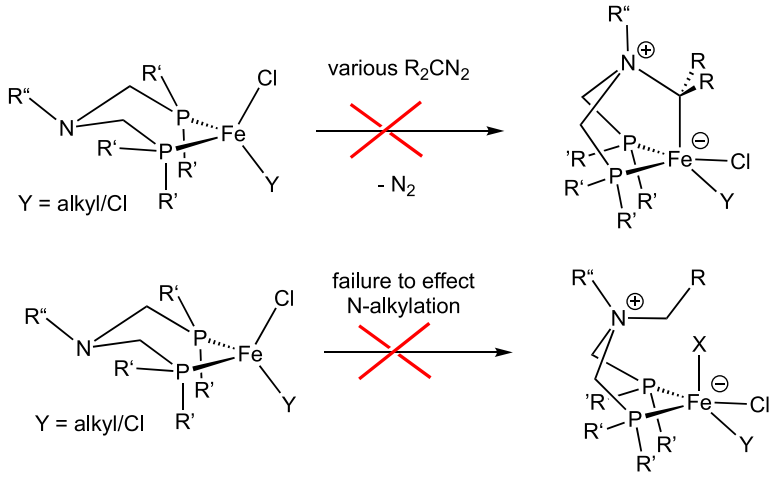

Scheme 7. Alkylidene transfer failed with Ph_2CN_2 and all variants. Aziridine Ad-^{c}CHN$_2$ [34] and PhCHN$_2$ were also applied to selected species, albeit unsuccessfully. All *N*-alkylation attempts also failed.

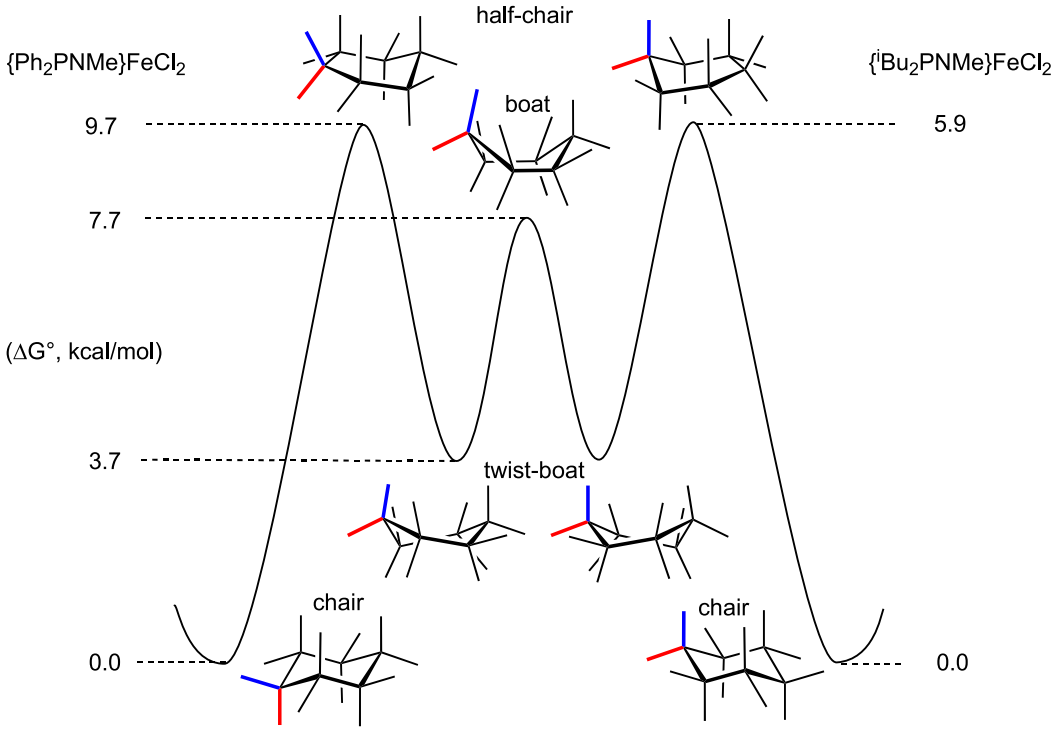

Fig. 5. Calculated conformational chair-to-boat calculations, shown ideally.

a ν(CO) of 1599 cm^{-1} corresponding to the acyl, were accompanied by a ^{1}H NMR spectrum of a diamagnetic complex, providing clear indication of inclusion of three carbonyls to afford the 18e$^-$ complex, {(^{i}Bu$_2$PCH$_2$)$_2$N^{t}Bu}(CO)$_2$FeCl(CO^{neo}Pe) (**8**). Overcarbonylation of related alkyls was similarly observed despite attempts to control stoichiometry.

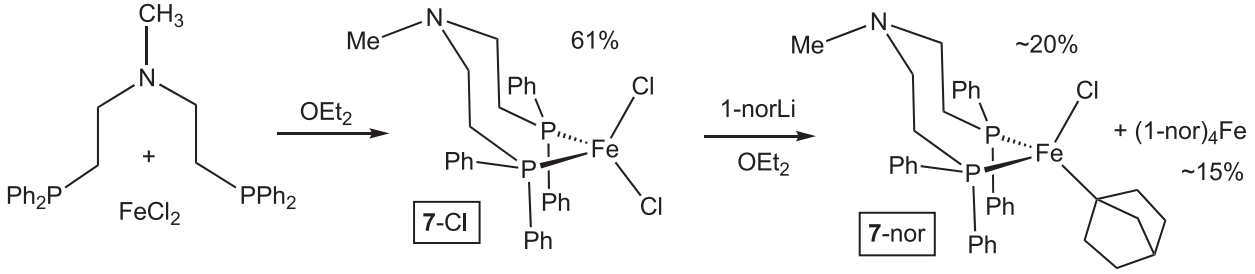

Scheme 8. Synthesis of {($Ph_2PCH_2CH_2$)$_2$N^{t}Bu}FeCl$_2$ (**7**-Cl) and {($Ph_2PCH_2CH_2$)$_2$N^{t}Bu}FeCl(1-nor) (**7**-nor).

Fig. 6 illustrates a molecular view of acyl {($^{i}Bu_2PCH_2)_2N^{t}Bu$}$(CO)_2FeCl(CO^{neo}Pe)$ (**8**), with the acyl opposite one carbonyl and the PNP ligand opposing the chloride and another CO. The stronger *trans*-influence of CO vs. Cl is revealed by d(FeP2) = 2.2890(3) Å being slightly greater than the d(FeP1) of 2.2273(3) Å. The configuration of the PNP ligand has completely changed from the T_d derivatives, as P1, P2, the methylene carbons, and iron are essentially planar, resulting in an out-of-plane nitrogen. The core angles of the pseudo octahedron are remarkably regular despite the ligand variation, averaging 90.1(35)°, and ranging from 84.95(4)° (P2-Fe-C3) to 96.688(12)°, the latter corresponding to the relatively splayed P-Fe-P angle. The remaining core bonds are normal for a low spin Fe(II) complex.

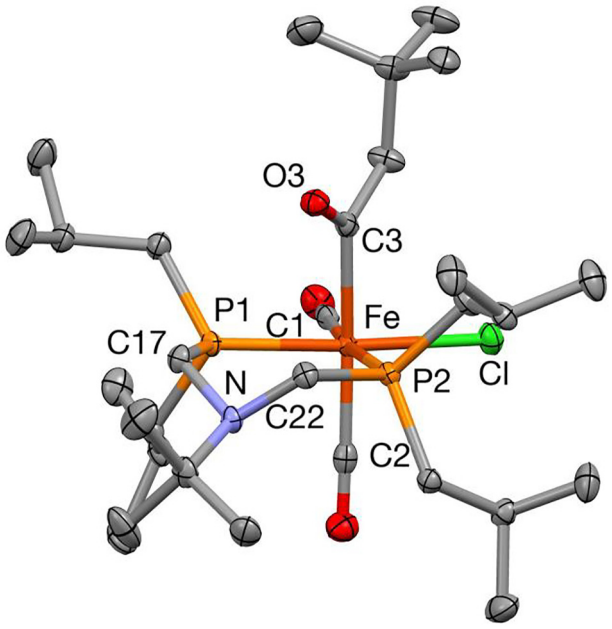

Fig. 6. Molecular view of {($^{i}Bu_2PCH_2)_2N^{t}Bu$}$(CO)_2FeCl(CO^{neo}Pe)$ (**8**); ellipsoids at 50%. Core interatomic distances (Å) and angles (°): FeCl, 2.3597(3); FeP1, 2.2273(3); FeP2, 2.2890(3); FeC1, 1.8126(14); FeC2, 1.8359(14); FeC3, 2.0296(13); Cl-Fe-P1, 175.725(14); Cl-Fe-P2, 86.562(12); Cl-Fe-C1, 86.80(4); Cl-Fe-C2, 91.16(4); Cl-Fe-C3, 91.83(4); P1-Fe-P2, 96.688(12); P1-Fe-C1, 89.82(4); P1-Fe-C2, 91.67(4); P1-Fe-C3, 85.71(4); P2-Fe-C1, 172.89(4); P2-Fe-C2, 89.15(4); P2-Fe-C3, 84.95(4); C1-Fe-C2, 93.54(6); C1-Fe-C3, 92.72(5); C2-Fe-C3, 173.21(5).

2.6. Synthesis and structure of {($Ph_2PCH_2CH_2)_2N^{t}Bu$}Fe ((H_2C = $CHSiMe_2)_2O$)

Successful efforts at preparing Fe(V) and Fe(IV) diimido complexes by Deng [49] and Power [50] utilized Fe(I) and Fe(0) starting materials, respectively, with adamantyl azide. Using {(Ph_2PCH_2-$CH_2)_2N^{t}Bu$}$FeCl_2$ (**1a**-Cl), reduction with KC_8 in the presence of bis-vinyldimethylsilyl-ether (dvtms) afforded {($Ph_2PCH_2CH_2)_2N^{t}$-Bu}-Fe((H_2C=$CHSiMe_2)_2O$) (**9**) in 93% yield as a green powder. An Evans' method measurement was consistent with an intermediate spin (S = 1) center, as μ_{eff} = 3.1 μ_B. Calculations showed the S = 1 state to be well below the singlet (S = 0, +12.3 kcal/mol). Unfortunately, exposure of **9** to various oxidizing alkylidene equivalents, namely diazo derivatives, failed to yield new complexes, and most were simply unreactive until decomposition. No evidence of 2 + 2 chemistry with the vinyl-silane functionalities could be discerned.

Crystals of {($Ph_2PCH_2CH_2)_2N^{t}Bu$}Fe((H_2C=$CHSiMe_2)_2O$) (**9**) were grown from pentane, and a molecular view of the formally Fe(0) complex is illustrated in Fig. 7. As expected, **9** is a highly distorted tetrahedron with the olefin centroids taken as two sites. The phosphorus atoms are constrained at 91.958(14)° apart due to the chelate, which is in a shallow boat configuration, and phosphine-olefin centroid angles vary from 102.89° to 126.74°. The dvtms ligand is asymmetric, with one olefin (C31-C32) essentially in a plane with the iron and nitrogen, and C37-C8 effectively perpendicular to that plane. This conformation renders the ether oxygen on the P1-side of the pseudo-tetrahedron. The iron-phosphine distances are more in line (2.2655(4), 2.2780(4) Å) with the previous high spin cases, and the olefin CC distances are typical for first row complexes that bind mostly via electrostatics [51].

3. Conclusions

3.1. Synthetic approach

The successful synthesis of a variety of PNP iron dihalides, alkylhalides and dialkyls was accomplished, yet none became the desired platform for a masked alkylidene in zwitterionic form, as planned via Scheme 3. Failure to alkylate at nitrogen, which has to be done after complexation due to competing P-alkylation, was a surprising impediment to subsequent heterolytic CH bond activation or reductive coupling. The orientation of the trisubstituted amine is inconsequential, as the inversion of the chelate ring does not have a prohibitive barrier. It may be that conditions under which alkylation can occur render the complexes susceptible to decomposition, as the weak fields of the pseudo tetrahedral complexes permit ready chelate arm dissociation. An obvious consequence of this factor is that P-alkylation is sometimes observed. If alkylation needs to proceed via an initial Lewis acid interaction of RX with the iron center, the site of binding, and the approach of the internal nucleophile could simply be unfavorable under conditions where the chelate is stable.

Previous failures in generating olefin metathesis capability at Fe (IV) complexes [20–22] that possess strong fields (*vide supra*) prompted the switch to lower coordination number, as exemplified by Scheme 1 and the attempts denoted herein, and supported by calculations.[52] It must also be assumed that the Deng [32,49] and Power [50] groups among others have been equally unsuccessful in generating alkylidene species capable of olefin metathesis, given their penchant and success at investigating 1st row transition metal ligand multiple bonds. What factor(s) is dominating the lack of generating an Fe(IV)=CRR′ moiety capable of 2 + 2 chemistry?

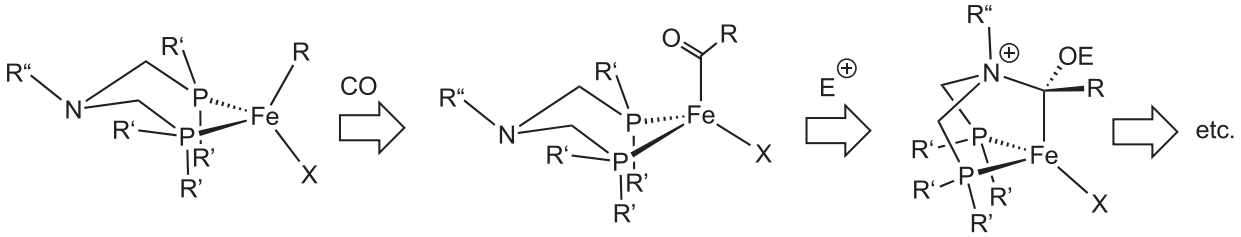

Scheme 9. Conceptual conversion of an acyl to masked carbene.

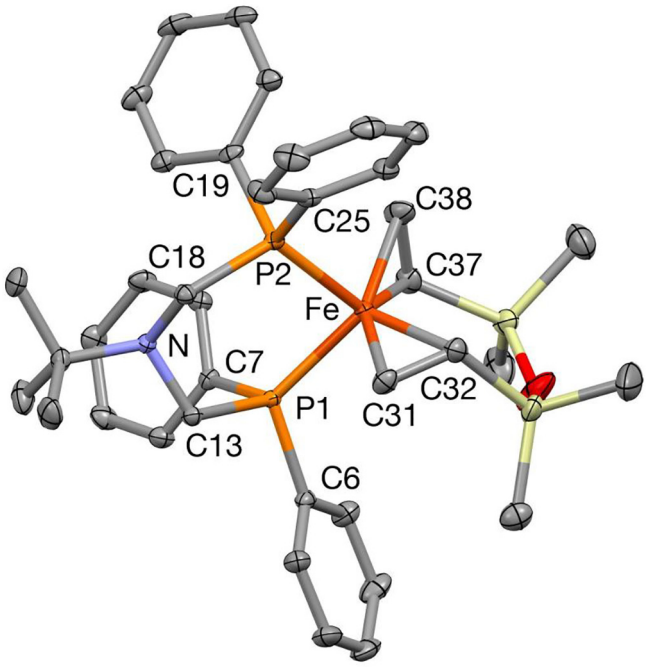

Fig. 7. Molecular view of {$(Ph_2PCH_2CH_2)_2N^tBu$}Fe($(H_2C{=}CHSiMe_2)_2O$) (**9**); ellipsoids at 50%. Core interatomic distances (Å) and angles (°): FeP1, 2.2655(4); FeP2, 2.2780 (4); FeC31, 2.1213(15); FeC32, 2.0628(15); FeC37, 2.0881(15); FeC38, 2.0540(16); C31-C32, 1.417(2); C37-C38, 1.413(2); P1-Fe-P2, 91.958(14); P1-Fe-C31, 88.08(5); P1-Fe-C32, 117.71(5); P1-Fe-C37, 99.01(5); P1-Fe-C38, 126.20(6); P2-Fe-C31, 88.73 (4); P2-Fe-C32, 111.76(5); P2-Fe-C37, 126.59(5); P2-Fe-C38, 93.20(5); C31-Fe-C32, 39.56(6); C31-Fe-C37, 143.30(6); C31-Fe-C38, 145.51(7); C32-Fe-C37, 108.53(7); C32-Fe-C38, 109.61(7), C37-Fe-C38, 39.89(7).

3.2. Are Fe(IV) olefin metathesis catalysts plausible?

Covalency is typically defined as "atoms sharing a pair of electrons", a statement that if not nebulous, is certainly broadly defined. In support, this simple statement regarding a common type of chemical bond is at least understandable in contrast to some recent definitions.[53] Perhaps a readily understood construct that can represent covalency is the overlap integral, which at least has intrinsic components of energy and overlap.

The best rationale for lack of metathesis activity infers a lack of covalency in the iron-carbon interaction, more specifically the π-bond, but exactly why covalency may be critical to metathesis is less transparent. To gain perspective, consider the interaction of a metal dπ orbital and its interaction with the corresponding carbon π-orbital. At the crux of this interaction is a 3d orbital that is small with respect to the 2p orbital of carbon, leading to two limiting cases of weak overlap, and one of potentially maximum covalence, as illustrated in Fig. 7.

In the normal configuration, the 2p orbital is well below the 3d, resulting in carbanion character in the M = CRR′ bond. Early metal 2nd row olefin metathesis catalysts possess this polar covalent interaction, as evidenced by reactions with electrophiles and Wittig-like reactivity [1,2]. At the other extreme, in an inverted field [54–57], cationic character of the alkylidene is intrinsic to the orbital ordering [22], leading to potential carbocation transfers, likely observed as cyclopropanations. It is the covalent representation that invites scrutiny, as it may provide the key to generating an active metathesis catalyst. The π-interaction may be interpreted within the framework of the 2-orbital, 2-electron, 4-state paradigm first utilized in assessing dihydrogen [58], and later applied to dimolybdenum δ- [59,60] and π-bonds [61]. For weak overlap situations, such as Chirik's and Deng's [14,32], the model of antiferromagnetic coupling (e.g. $Fe^{\uparrow}(III)(\text{-}C^{\downarrow}Ar_2)$) has been used as an alternative to a bond, in part based on chemical reactivity, as cyclopropanations are observed. In these weak overlap situations, the GS is not necessarily covalent, as the overlap integral is so small that substantial ionic character contributes. If ϕ_M and ϕ_L deviate in the slightest, the ionic character can become dominant, likely leading to cyclopropanation.

On the left in Fig. 8 is the standard strong overlap case where olefin metathesis occurs, and the only electrons in the plane of the metalacyclobutane originate from the M=C and C=C π-bonds. Note that the total energies of the Ψ^b and CCπ^b orbitals' electrons are shown roughly the same as Ψ^b_S and Ψ^b_A ensuring that each component of the catalytic cycle is similar. Strong covalent interactions result in excellent M/C and C/C overlap in metallacycle formation, and that the symmetric (S) and antisymmetric (A) orbitals reveal the two new bonds (see Fig. 9).

Assume the weak overlap "covalent" situation actually results in an interaction that has substantial ionic character. Fig. 8 shows that the combination of poor orbital overlap, in part due to energy mismatches between metal and carbon double bond orbitals, and also due to the ionic character of the orbitals, presents significant problems. In the worst case, if the interaction is weak enough, the requisite Ψ^b_A orbital may not even be populated, as Ψ^*_S may be filled instead, resulting in no net bonding. The asymmetry in the ground state of the alkylidene clearly impacts overlap, and cyclopropanation is a likely consequence.

The problem is deceptively simple, as the coordination sphere must be strongly donating enough to engender low spin derivatives covalent enough to undergo metalacyclobutane formation [52], yet low coordination environments are affiliated with weak field, high spin systems, except under extraordinary circumstances. Energies of the metal dπ orbital and carbon 2pπ orbital must be closely matched to elicit as much covalence as possible in the alkylidene. Second, the alkylidene must be electronically oxidizing enough to share the π-electrons with the iron, a factor that is difficult for all first-row transition metals, especially the later ones.[62] To what extent geometric considerations, such as the shorter M−C bonds in the first row, contribute to metalacyclobutane formation and its rearrangement are unknown. It may be necessary to turn toward anionic iron(IV) derivatives to expand the 3d orbitals such that appropriate π-overlap between iron and carbon can be achieved, albeit with the introduction of a new problem, that of increased electron–electron repulsions.

4. Experimental

4.1. General considerations

All manipulations were performed using either glovebox, Schlenk, or high vacuum line techniques, unless stated otherwise. All glassware was oven dried at 180 °C·THF and ether were distilled under nitrogen from purple sodium benzophenone ketyl and vacuum transferred from the same prior to use. Hydrocarbon solvents were treated in the same manner with the addition of 1–2 mL/L tetraglyme. Benzene d_6 was dried over sodium, vacuum transferred and stored over sodium·THF-d_8 was dried over sodium, and vacuum transferred from sodium benzophenone ketyl prior to use. Acetonitrile d_3 was dried over refluxing CaH_2, vacuum distilled and stored over CaH_2, and chloroform d_1 (Cambridge Isotope Laboratories) was used as received. PNP ligands were prepared via literature preparations [35–40].

NMR spectra were obtained using Varian 300 MHz (Mercury), 400 MHz (Inova), 500 MHz (Inova) and 600 MHz (Inova) spectrometers. ^1H and ^{13}C NMR shifts are referenced to benzene d_6 (^1H, δ7.16 ppm; ^{13}C, δ128.39 ppm), toluene d_8 (^1H, δ2.09 ppm; ^{13}C,

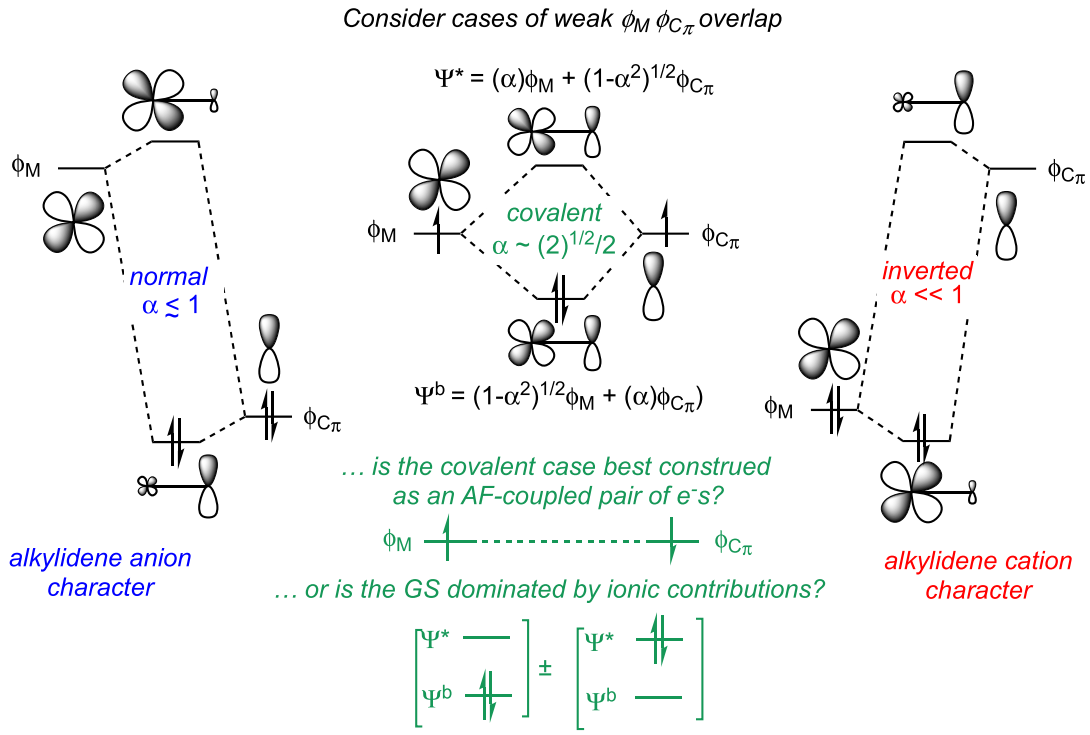

Fig. 8. Normal, covalent, and inverted field combinations of a 1st row transition metal dπ orbital and a carbon 2pπ orbital.

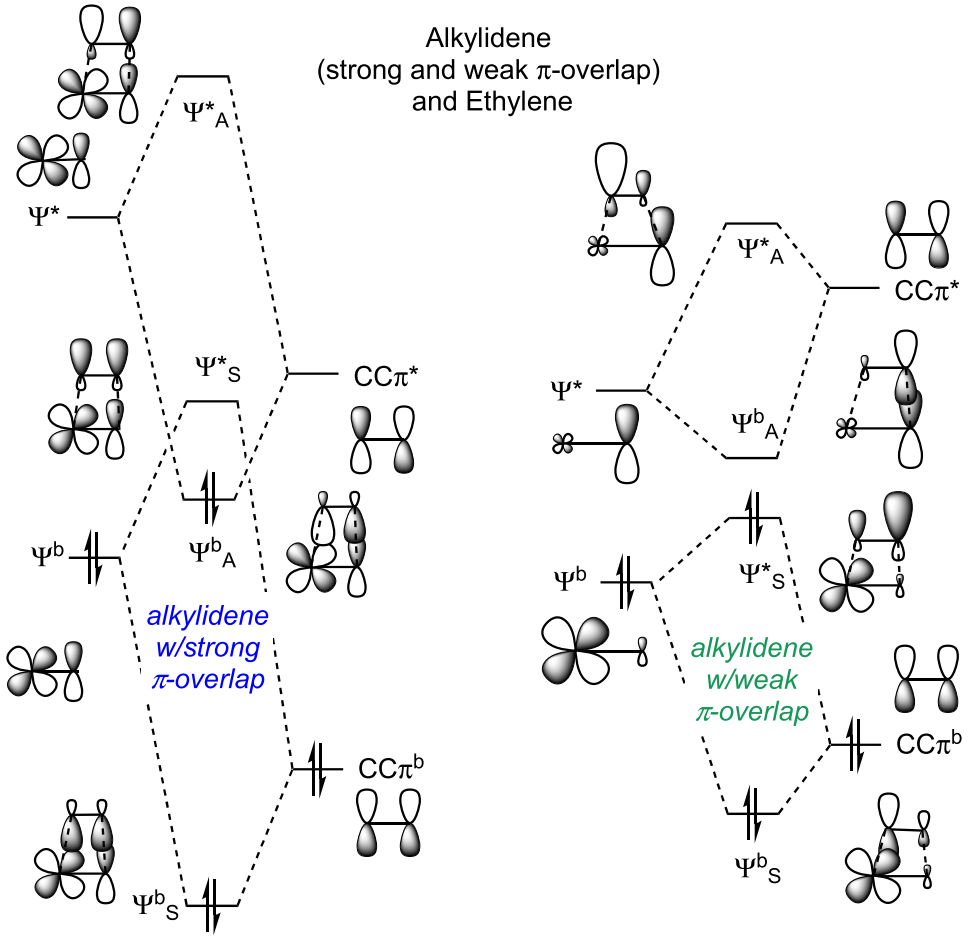

Fig. 9. The generation of a metalacyclobutane via alkylidenes (strong and weak) and an ethylene.

δ20.40 ppm), acetonitrile d_3 (^{1}H, δ1.94 ppm; ^{13}C, δ118.26 ppm), tetrahydrofuran d_8 (^{1}H, δ3.58 ppm; ^{13}C, δ67.57 ppm), dichloromethane d_2 (^{1}H, δ5.32 ppm; ^{13}C, δ53.84 ppm), deuterium oxide (^{1}H, δ4.79 ppm; ^{13}C, CH_3CN spike, δ1.79 ppm). Solution magnetic measurements were conducted via Evans' method in the same solvent as the ^{1}H NMR was conducted.[43] Elemental analyses were performed by Robertson Microlit Laboratories, Madison, New Jersey.

4.2. Procedures

4.2.1. {($Ph_2PCH_2)_2N^tBu$}$FeCl_2$ (**1a**-Cl)

To a 100 mL round bottom flask charged with anhydrous $FeCl_2$ (0.964 g, 7.61 mmol) and $(Ph_2PCH_2)_2N^tBu$ (3.929 g, 8.37 mmol) was added 50 mL of freshly distilled THF at −78 °C. The reaction mixture was allowed to warm slowly to 23 °C and stirred for 16 h, resulting in a yellow solution. The volatiles were evaporated, and the yellow residue was triturated with pentane (2 × 10 mL). The residue was suspended in pentane, filtered, and washed (2 × 10 mL) to isolate the yellow powder (4.159 g, 92%). ^{1}H NMR (C_6D_6) δ -3.68 (7H), 2.67 (14H), 8.11 (2H), 14.92 (10*H*). μ_{eff} (Evans) = 5.6 μ_B. Anal. for $C_{30}H_{33}P_2NFeCl_2$ (calc.) C 60.43, H 5.58, N 2.35; (found) C 59.73, H 5.51, N 2.21.

4.2.2. {($Ph_2PCH_2)_2N^tBu$}$FeBr_2$ (**1a**-Br)

To a 50 mL round bottom flask charged with anhydrous $FeBr_2$ (130 mg, 0.603 mmol) and $(Ph_2PCH_2)_2N^tBu$ (300 mg, 0.639 mmol) was added 20 mL of freshly distilled THF at −78 °C. The reaction mixture was allowed to warm slowly to 23 °C and stirred for 16 h, resulting in a yellow solution. The volatiles were evaporated, and the residue was triturated with pentane (2 × 10 mL). The residue was suspended in pentane, filtered, and washed (2 × 10 mL) to isolate the pale yellow powder (366 mg, 85%). ^{1}H NMR (C_6D_6) δ -3.54 (6H), 2.89 (14H), 15.10 (13H). μ_{eff} (Evans) = 5.5 μ_B.

4.2.3. {($Ph_2PCH_2)_2NMe$}$FeCl_2$ (**1b**-Cl)

To a 100 mL round bottom flask charged with anhydrous $FeCl_2$ (0.287 g, 2.26 mmol) and $(Ph_2PCH_2)_2N^tBu$ (1.061 g, 2.48 mmol) was added 50 mL of freshly distilled THF at −78 °C. The reaction mixture was allowed to warm slowly to 23 °C and stirred for 16 h, resulting in a yellow solution. The volatiles were evaporated, and the residue was triturated with pentane (2 × 10 mL). The residue was suspended in pentane, filtered, and washed (2 × 10 mL) to isolate the yellow powder (1.179 g, 87%). Crystals suitable for X-ray diffraction were obtained via slow evaporation of a concentrated THF solution at 23 °C. ^{1}H NMR (THF-d_8) δ -2.59 (6H), -1.86 (5H), 5.20 (4H), 14.30 (12H). μ_{eff} (Evans) = 5.2 μ_B. Anal. for $C_{27}H_{27}P_2NFeCl_2$ (calc.) C 58.51, H 4.91, N 2.53; (found) C 57.30, H 4.79, N 2.27.

4.2.4. {($^iBu_2PCH_2)_2N^tBu$}$FeCl_2$ (**2a**-Cl)

To a 100 mL round bottom flask charged with anhydrous $FeCl_2$ (1.498 g, 11.82 mmol) and $(^iBu_2PCH_2)_2N^tBu$ (5.00 g, 12.83 mmol) was added 50 mL of freshly distilled Et_2O at −78 °C. The reaction mixture was allowed to warm slowly to 23 °C and stirred for 16 h, resulting in a pale yellow solution with a white suspension. The volatiles were evaporated, and the off-white residue was triturated with pentane (2 × 10 mL). The residue was suspended in pentane, filtered, and washed (2 × 10 mL) to isolate the off-white powder (5.806 g, 89%). crystals suitable for X-ray diffraction were grown from slow evaporation of a concentrated pentane solution at −35 °C. ^{1}H NMR (C_6D_6) δ -1.57 (18H), 1.45 (13H), 2.84 (18H) μ_{eff} (Evans) = 5.0 μ_B. Anal. for $C_{22}H_{49}P_2NFeCl_2$ (calc.) C 51.18, H 9.57, N 2.71; (found) C 51.45, H 9.82, N 2.71.

4.2.5. {($^iBu_2PCH_2)_2NMe$}$FeCl_2$ (**2b**-Cl)

To a 100 mL round bottom flask charged with anhydrous $FeCl_2$ (0.693 g, 5.47 mmol) and $(^iBu_2PCH_2)_2NMe$ (1.920 g, 5.53 mmol) was added 50 mL of freshly distilled THF at −78 °C. The reaction mixture was allowed to warm slowly to 23 °C and stirred for 16 h, resulting in a pale yellow solution. The volatiles were evaporated, and the off-white residue was triturated with pentane (2 × 10 mL) and then with Et_2O (3 × 10 mL). Taking the residue up in Et_2O, cooling the solution to −78 °C followed by filtering the solution yields a white powder (1.778 g, 69%). ^{1}H NMR (THF-d_8) δ -0.89 (23H), 48.98 (10*H*), 122.54 (10*H*). μ_{eff} (Evans) = 5.6 μ_B.

4.2.6. {($R'_2PCH_2)_2NR''$}FeR(Y) general procedure

To a 50 mL round bottom flask charged with {$(R'_2PCH_2)_2NR''$} $FeCl_2$ (0.287 g, 2.26 mmol) and one or two equivalents of RLi was added 25 mL of freshly distilled Et_2O at −78 °C. The reaction mixture was allowed to warm slowly to 23 °C and stirred for 16 h. The solution was filtered, and the volatiles evaporated. Taking the residue up in minimal pentane, cooling the solution to −78 °C followed by filtering yields a microcrystalline solid.

*4.2.6.1. {($Ph_2PCH_2)_2N^tBu$}FeCl(1-nor) (**3a**-nor).* ^{1}H NMR (C_6D_6) δ -9.76 (2H), -5.61 (3H), -2.31 (3H), 3.12 (17H), 11.41 (6H), 14.84 (1H), 15.56 (6H), 19.10 (2H), 34.27 (3H), 64.75 (1H). μ_{eff} (Evans) = 5.1 μ_B. Anal. for $C_{37}H_{44}P_2NFeCl$ (calc.) C 67.74, H 6.76, N 2.14; (found) C 66.51, H 6.82, N 1.80.

*4.2.6.2. {($Ph_2PCH_2)_2N^tBu$}FeCl(^{neo}Pe) (**3a**-^{neo}Pe).* ^{1}H NMR (C_6D_6) δ -4.37 (3H), -4.24 (3H), -3.65 (1H) 2.69 (3H), 3.37 (12H), 10.81 (6H), 14.92 (2H), 15.85 (5H), 39.90 (9H). μ_{eff} (Evans) = 5.6 μ_B.

*4.2.6.3. {($Ph_2PCH_2)_2N^tBu$}FeCl(CH_2SiMe_3) (**3a**-CH_2SiMe_3).* ^{1}H NMR (C_6D_6) δ -4.23 (6H), 2.62 (12H), 12.55 (17H), 15.51 (9H). μ_{eff} (Evans) = 5.2 μ_B.

*4.2.6.4. {($Ph_2PCH_2)_2NMe$}FeCl(1-nor) (**3b**-nor).* ^{1}H NMR (C_6D_6) δ -4.73 (1H), -2.91 (1H), 2.77 (16H), 3.44 (16H), 9.66 (2H), 15.39 (2H). μ_{eff} (Evans) = 5.3 μ_B.

*4.2.6.5. {($Ph_2PCH_2)_2NMe$}FeCl(CH_2SiMe_3) (**3b**-CH_2SiMe_3).* ^{1}H NMR (C_6D_6) δ -5.24 (3H), -3.56 (3H), 2.66 (3H), 3.36 (3H), 4.60 (3H), 7.46 (6H), 10.19 (4H), 16.11 (13H). μ_{eff} (Evans) = 5.6 μ_B.

*4.2.6.6. {($^iBu_2PCH_2)_2N^tBu$}FeCl(1-nor) (**4a**-nor).* ^{1}H NMR (C_6D_6) δ -12.67 (4H), -7.25 (9H), -5.53 (10*H*), -3.88 (10*H*), 4.68 (17H), 19.89 (3H), 35.67 (4H), 62.06 (1H), 99.74 (2H). μ_{eff} (Evans) = 4.7 μ_B. Crystals suitable for X-ray diffraction were grown from slow evaporation of a concentrated pentane solution at −35 °C.

*4.2.6.7. {($^iBu_2PCH_2)_2N^tBu$}FeCl(^{neo}Pe) (**4a**-^{neo}Pe).* ^{1}H NMR (C_6D_6) δ -5.86 (11*H*), -4.22 (9H), -2.68 (9H), 1.37 (15H), 16.66 (2H), 37.81 (10*H*). μ_{eff} (Evans) = 4.8 μ_B.

*4.2.6.8. {($^iBu_2PCH_2)_2N^tBu$}FeCl(CH_2SiMe_3) (**4a**-CH_2SiMe_3).* ^{1}H NMR (C_6D_6) δ -5.56 (8H), -3.86 (9H), -2.63 (8H), 3.03 (8H), 3.84 (16H) 14.99 (11*H*). μ_{eff} (Evans) = 5.4 μ_B.

*4.2.6.9. {($^iBu_2PCH_2)_2NMe$}FeCl(1-nor) (**4b**-nor).* ^{1}H NMR (C_6D_6) δ -6.64 (10H), -5.21 (8H), -0.66 (17H), 3.91 (3H), 18.76 (3H), 34.20 (4H), 46.74 (3H), 61.57 (2H), 67.29 (2H), 81.74 (2H). μ_{eff} (Evans) = 5.1 μ_B

*4.2.6.10. {($^iBu_2PCH_2)_2NMe$}FeCl(CH_2SiMe_3) (**4b**-CH_2SiMe_3).* ^{1}H NMR (C_6D_6) δ -9.21 (1H), -5.34 (7H), -3.31 (6H), -0.74 (7H), 2.82 (8H), 3.57 (8H), 15.13 (11H), 21.84 (1H), 70.69 (1H), 79.29 (2H), 105.74 (2H). μ_{eff} (Evans) = 5.1 μ_B.

*4.2.6.11. {($Ph_2PCH_2)_2N^tBu$}Fe(^{neo}Pe)$_2$ (**5a**-^{neo}Pe).* ^{1}H NMR (C_6D_6) δ -4.25 (10H), 2.52 (17H), 15.08 (13H), 28.18 (15H). μ_{eff} (Evans) = 5.3 μ_B. Anal. for $C_{40}H_{55}P_2NFe$ (calc.) C 71.96, H 8.30, N 2.10; (found) C 70.57, H 8.26, N 1.92.

*4.2.6.12. {($^iBu_2PCH2)_2N^tBu$}Fe(1-nor)$_2$ (**6a**-nor).* ^{1}H NMR (C_6D_6) δ -4.32 (11 H), -1.59 (2H), 1.58 (21H), 16.67 (13H), 28.42 (6H), 51.99 (2H). μ_{eff} (Evans) = 5.5 μ_B.

*4.2.7. {($^iBu_2PCH_2)_2N^tBu$}(CO)$_2$FeCl($CO^{neo}Pe$) (**8**)*

To a 25 mL round bottom charged with 4a (50 mg, 0.097 mmol) was added 10 mL freshly distilled C_6H_6. The flask was allowed to warm to room temperature and under 1 atm of CO. An immediate color change was observed, the solution was stirred for 16 h. The volatiles were removed, and the residue was washed with pentane (2 × 10 mL), and removed to give an orange powder. The volatiles were evaporated to give an orange powder. Orange crystals suitable for X-ray diffraction were grown from slow evaporation of a concentrated Et_2O solution at −35 °C. IR nujol mull ν(CO) 2009 cm^{-1}, 1954 cm^{-1}, (acyl) 1599 cm^{-1}. ^{1}H NMR (C_6D_6) δ 0.80 (s, 9H N^tBu-CH_3), {0.90, 0.90, 0.92, 0.95, 0.98, 1.00, 1.13, 1.14 (24H ^iBu-CH_3)}, 1.25 (s, 9H ^{neo}Pen-CH_3), {1.94, 1.99, 2.01, 2.06 (m, 4H ^iBu-CH)}, {1.62, 1.84, 1.85, 1.88, 2.02, 2.24, 2.47, 2.58 (8H ^iBu-CH_2)}, {2.94, 3.01, 3.09, 3.12 (4H, PCH_2N)}, {3.64, 4.13 (d, *J* = 18.01 Hz 2H ^{neo}Pen-CH_2)}. ^{13}C NMR (C_6D_6) {24.47, 25.24, 25.25, 25.39, 25.64, 26.65, 25.87, 26.41 (^iBu-CH_3)}, 26.29 (N^tBu-CH_3), 29.78 (^{neo}Pen-CH_3), {30.00, 30.66, 31.54, 32.50 (^iBu-$CH(CH_3)_2$)}, 32.45 (^{neo}Pen-$C(CH_3)_3$), {33.48, 34.67, 36.66, 37.37 (^iBu-CH_2)}, {47.15, 47.77 (PCH_2N)}, 56.57 (N^tBu-$C(CH_3)_3$), 71.94 (^{neo}Pen-CH_2), 185.00 (acyl) {212.57, 212.92 (CO)}.

*4.2.8. {($Ph_2PCH_2CH_2)_2N^tBu$}Fe((H_2C = $CHSiMe_2)_2O$) (**9**)*

To a 50 mL two necked flask charged with {($Ph_2PCH_2)_2N^tBu$}$FeCl_2$ (315 mg, 0.528 mmol) and 1,3-Divinyltetramethyldisiloxane (100 mg, 0.536 mmol) and equipped with a solid addition finger charged with KC_8 (152 mg, 1.12 mmol) was added 20 mL freshly distilled THF at −78 °C. The KC_8 was added at −78 °C and the reaction mixture was allowed to warm slowly to 23 °C and stirred for 16 h. The volatiles were evaporated, the residue was taken up in pentane and filtered through a silica plug to give a green solution. The volatiles were evaporated to give a green powder (0.351 g, 93%). ^{1}H NMR (C_6D_6) δ -7.85 (1H), -1.87 (5H), -0.99 (1H), 0.66 (8H), 0.95 (8H), 1.38 (13H), 4.06 (1H), 9.98 (9H), 11.78 (3H), 13.25 (1H), 31.70 (1H). μ_{eff} (Evans) = 3.1 μ_B. Crystal suitable for x-ray diffraction were grown from slow evaporation of a concentrated pentane solution at −35 °C.

4.3. X-ray crystal structure determinations

*4.3.1. {($Ph_2PCH_2)_2NMe$}$FeCl_2$ (**1b**-Cl)*

A yellow plate measuring 0.46 × 0.15 × 0.09 mm^3 was obtained from THF. Crystal data for $C_{27}H_{27}Cl_2NP_2Fe$, M = 554.18, monoclinic, $P2_1/c$, a = 14.72110(10), b = 11.06180(10), c = 16.53250(10) Å, β = 96.0520(10)°, V = 2677.18(3) Å^3, T = 173(2)K, λ = 1.54184 Å, Z = 4, ρ_{calc} = 1.375 Mg/m^3, μ = 7.599 mm^{-1}, 108,554 reflections, 5702 independent (R_{int} = 0.0562), R_1 (all data) = 0.0305, wR_2 = 0.0816, R_1 (I > 2σI) = 0.0295, wR_2 = 0.0808, GOF = 1.096.

*4.3.2. {($^iBu_2PCH_2)_2N^tBu$}$FeCl_2$ (**2a**-Cl)*

A yellow plate measuring 0.24 × 0.08 × 0.07 mm^3 was obtained from pentane. Crystal data for $C_{22}H_{49}Cl_2NP_2Fe$, M = 516.31, monoclinic, $P2_1/n$, a = 11.36310(10), b = 15.32800(10), c = 16.79070(10) Å, β = 94.2580(10)°, V = 2916.43(3) Å^3, T = 222(2)K, λ = 1.54184 Å, Z = 4, ρ_{calc} = 1.176 Mg/m^3, μ = 6.916 mm^{-1}, 123,225 reflections, 5538 independent (R_{int} = 0.0581), R_1 (all data) = 0.0270, wR_2 = 0.0714, R_1 (I > 2σI) = 0.0257, wR_2 = 0.0706, GOF = 1.059.

*4.3.3. {($^iBu_2PCH_2)_2N^tBu$}FeCl(1-nor) (**4a**-nor)*

A yellow plate measuring 0.26 × 0.11 × 0.07 mm^3 was obtained from pentane. Crystal data for $C_{29}H_{60}ClNP_2Fe$, M = 576.02, monoclinic, $P2_1/n$, a = 9.91359(4), b = 24.79084(8), c = 13.98973(6) Å, β = 106.1234(4)°, V = 3302.96(2) Å^3, T = 100(2)K, λ = 1.54184 Å, Z = 4, ρ_{calc} = 1.158 Mg/m^3, μ = 5.428 mm^{-1}, 147,953 reflections, 7066 independent (R_{int} = 0.0409), R_1 (all data) = 0.0281, wR_2 = 0.0744, R_1 (I > 2σI) = 0.0276, wR_2 = 0.0740, GOF = 1.053.

*4.3.4. {($^iBu_2PCH_2)_2N^tBu$}(CO)$_2$FeCl($CO^{neo}Pe$) (**8**)*

An orange block measuring 0.29 × 0.25 × 0.11 mm^3 was obtained from diethyl ether. Crystal data for $C_{30}H_{60}ClNO_3P_2Fe$, M = 636.03, monoclinic, $P2_1/n$, a = 11.92710(10), b = 18.0981(2), c = 16.6852(2) Å, β = 93.1790(10)°, V = 3594.30(7) Å^3, T = 100(2) K, λ = 0.71073 Å, Z = 4, ρ_{calc} = 1.175 Mg/m^3, μ = 0.611 mm^{-1}, 84,638 reflections, 8892 independent (R_{int} = 0.0356), R_1 (all data) = 0.0345, wR_2 = 0.0724, R_1 (I > 2σI) = 0.0285, wR_2 = 0.0692, GOF = 1.032.

*4.3.5. $Ph_2PCH_2CH_2)_2N^tBu$}Fe((H_2C = $CHSiMe_2)_2O$) (**9**)*

An orange block measuring 0.29 × 0.25 × 0.11 mm^3 was obtained from pentane. Crystal data for $C_{38}H_{51}NOP_2Si_2Fe$, M = 711.76, triclinic, P1bar, a = 10.61500(10), b = 12.73230(10), c = 15.6085(2) Å, α = 72.4270(10)°, β = 84.5660(10)°, γ = 68.3740 (10)° V = 1869.21(4) Å^3, T = 100(2)K, λ = 0.71073 Å, Z = 2, ρ_{calc} = 1.265 Mg/m^3, μ = 0.583 mm^{-1}, 77,875 reflections, 8244 independent (R_{int} = 0.0359), R_1 (all data) = 0.0347, wR_2 = 0.0799, R_1 (I > 2σI) = 0.0317, wR_2 = 0.0776, GOF = 1.035.

4.4. Computational methods

Computations described herein employed the Gaussian 16 code (revision A.03) [45]. The B3PW91 [46] functional with the GD3 empirical dispersion correction [47] was utilized in conjunction with the 6-31+G(d) basis set. Initial computations indicated a quintet ground state, so that unrestricted DFT methods were employed with no evidence of spin contamination as evidenced by inspection of the <S^2> expectation value. All minima and transition states were optimized with neither symmetry nor geometric constraint, and were verified for the correct number of imaginary frequencies via computation of the energy Hessian. All reported energetics assumed 1 atm and 298.15 K.

CRediT authorship contribution statement

Gregory M. George: Experimental. **Peter T. Wolczanski:** Conceptualization. **Samantha N. MacMillan:** X-ray crystallography. **Thomas R. Cundari:** Calculations.

Declaration of Competing Interest

The authors declare that they have no known competing financial interests or personal relationships that could have appeared to influence the work reported in this paper.

Acknowledgements

We thank Dr. Spencer P. Heins for initiating this work. Support from the National Science Foundation (CHE-1664580 (PTW), CHE-1464943 (TRC)) and Cornell University is gratefully acknowledged. NSF support for UNT CASCaM HPC cluster via CHE-1531468, and the CCB NMR facility (NSF-MRI CHE-1531632) is appreciated, as is technical aid from Ivan Keresztes.

Appendix A. Supplementary data

Supplementary data to this article can be found online at https://doi.org/10.1016/j.poly.2020.114460.

References

[1] H. Jeong, J.M. John, R.R. Schrock, A.H. Hoveyda, J. Am. Chem. Soc. 137 (2015) 2239–2242.
[2] (a) R.R. Schrock, Angew. Chem. Int. Ed. 45 (2006) 3748–3759;
(b) R.R. Schrock, A.H. Hoveyda, Angew. Chem. Int. Ed. 42 (2003) 4592–4633.
[3] V.M. Marx, A.H. Sullivan, M. Melaimi, S.C. Virgil, B.K. Keitz, D.S. Weinberger, G. Bertrand, R.H. Grubbs, Angew. Chem. Int. Ed. 54 (2015) 1919–1923.
[4] R.H. Grubbs, Angew. Chem. Int. Ed. 45 (2006) 3760–3765.
[5] Y. Chauvin, Angew. Chem. Int. Ed. 45 (2006) 3740–3747.
[6] M.P. Coles, V.C. Gibson, W. Clegg, M.R. Elsegood, P.A. Porrelli, Chem. Commun. (1996) 1963–1964.
[7] P. Wu, G.P.A. Yap, K.H. Theopold, J. Am. Chem. Soc. 140 (2018) 7088–7091.
[8] (a) M. Brookhart, J.R. Tucker, G.R. Husk, J. Am. Chem. Soc. 105 (1983) 258–264;
(b) M. Brookhart, J.R. Tucker, J. Am. Chem. Soc. 103 (1981) 979–981;
(c) M. Brookhart, D. Timmers, J.R. Tucker, G.D. Williams, G.R. Husk, H. Brunner, B. Hammer, J. Am. Chem. Soc. 105 (1983) 6721–6723.
[9] G. Poignant, S. Nlate, V. Guerchais, A.J. Edwards, P.R. Raithby, Organometallics 16 (1997) 124–132.
[10] V. Mahias, S. Cron, L. Toupet, C. Lapinte, Organometallics 15 (1996) 5399–5408.
[11] A. Klose, E. Solari, C. Floriani, N. Re, A. Chiesi-Villa, C. Rizzoli, Chem. Commun. (1997) 2297–2298.
[12] V. Esposito, E. Solari, C. Floriani, N. Re, C. Rizzoli, A. Chiesi-Villa, Inorg. Chem. 39 (2000) 2604–2613.
[13] Y. Li, J.-S. Huang, Z.-Y. Zhou, C.-M. Che, X.-Z. You, J. Am. Chem. Soc. 124 (2002) 13185–13193.
[14] S.K. Russell, J.M. Hoyt, S.C. Bart, C. Milsmann, S.C.E. Stieber, S.P. Semproni, S. DeBeer, P.J. Chirik, Chem Sci. 5 (2014) 1168–1174.
[15] (a) K.A.M. Kremer, G.-H. Kuo, E.J. O'Connor, P. Helquist, R.C. Kerber, J. Am. Chem. Soc. 104 (1982) 6119–6121;
(b) G.-H. Kuo, P. Helquist, R.C. Kerber, Organometallics 3 (1984) 806–808.
[16] T. Bodnar, A.R. Cutler, J. Organomet. Chem. 213 (1981) C31–C36.
[17] (a) A. Davison, J.P. Selegue, J. Am. Chem. Soc. 100 (1978) 7763–7765;
(b) R.D. Adams, A. Davison, J.P. Selegue, J. Am. Chem. Soc. 101 (1979) 7232–7238.
[18] M.I. Bruce, A.G. Swincer, Aust. J. Chem. 33 (1980) 1471–1483.
[19] C.P. Casey, W.H. Miles, H. Tukada, J.M. O'Connor, J. Am. Chem. Soc. 104 (1982) 3761–3762.
[20] B.M. Lindley, A. Swidan, E.B. Lobkovsky, P.T. Wolczanski, M. Adelhardt, J. Sutter, K. Meyer, Chem. Sci. 6 (2015) 4730–4736.
[21] B.M. Lindley, B.P. Jacobs, S.N. MacMillan, P.T. Wolczanski, Chem. Commun. 52 (2016) 3891–3894.
[22] B.P. Jacobs, R.G. Agarwal, P.T. Wolczanski, T.R. Cundari, Polyhedron 116 (2016) 47–56.
[23] J. Yamada, M. Fujiki, K. Nomura, Organometallics 24 (2005) 2248–2250.
[24] K. Nomura, S. Zhang, Chem. Rev. 111 (2011) 2342–2362.
[25] X. Hou, K. Nomura, Dalton Trans. 46 (2017) 12–24.
[26] (a) S.M. Rocklage, J.D. Fellmann, G.A. Rupprecht, L.W. Messerle, R.R. Schrock, J. Am. Chem. Soc. 103 (1981) 1440–1447;
(b) K.C. Wallace, A.H. Liu, J.C. Dewan, R.R. Schrock, J. Am. Chem. Soc. 110 (1988) 4964–4977.
[27] (a) F.N. Tebbe, G.W. Parshall, D.W. Ovenall, J. Am. Chem. Soc. 101 (1979) 5074–5075;
(b) U. Klabunde, F.N. Tebbe, G.W. Parshall, R.L. Harlow, J. Mol. Catal. 8 (1980) 37–51.
[28] T.R. Howard, J.B. Lee, R.H. Grubbs, J. Am. Chem. Soc. 102 (1980) 6876–6878.
[29] (a) Y.L. Qian, D.F. Zhang, J.L. Huang, H.Y. Ma, A.S.C. Chan, J. Molec. Catal. A 133 (1988) 135–138;
(b) J.F. Liu, D.F. Zhang, J.L. Huang, Y.L. Qian, A.S.C. Chan, J. Molec. Catal. A 142 (1999) 301–304;
(c) J.F. Liu, D.F. Zhang, J.L. Huang, Y.L. Qian, A.S.C. Chan, J. Polym. Sci. Par A. 38 (2000) 1639–1640.
[30] O. Eisenstein, R. Hoffmann, A.R. Rossi, J. Am. Chem. Soc. 103 (1981) 5582–5584.
[31] (a) H. M. L. Davies, E. G. Antoulinakis, "Intermolecular Metal-Catalyzed Carbenoid Cyclopropanations" in Organic Reactions, Ed. L. E. Overman, John Wiley & Sons: New York, 2001. (b) H. M. L. Davies, R. E. J. Beckwith, Chem. Rev. 103 (2003) 2861-2903.
[32] J. Liu, L. Hu, L. Wang, H. Chen, L. Deng, J. Am. Chem. Soc. 139 (2017) 3876–3888.
[33] (a) B.P. Jacobs, P.T. Wolczanski, Q. Jiang, T.R. Cundari, S.N. MacMillan, J. Am. Chem. Soc. 139 (2017) 12145–12148;
(b) T.R. Cundari, B.P. Jacobs, S.N. MacMillan, P.T. Wolczanski, Dalton Trans. 47 (2018) 6025–6030.
[34] S.R. Hare, M. Orman, F. Dewan, E. Dalchand, C. Buzard, S. Ahmed, J.C. Tolentino, U. Sethi, K. Terlizzi, C. Houferak, A.M. Stein, A. Stedronsky, D.M. Thamattoor, D. J. Tantillo, D.C. Merrer, J. Org. Chem. 80 (2015) 5049–5065.
[35] (a) C. Klemps, E. Payet, L. Magna, L. Saussine, X.F. Le Goff, P. Le Floch, Chem. Eur. J. 15 (2009) 8259–8268;
(b) K. Kellner, A. Tzschach, Z. Nagy-Magos, L. Markó, J. Organomet. Chem. 193 (1980) 307–314.
[36] M.R. DuBois, D.L. DuBois, Chem. Soc. Rev. 38 (2009) 62–72.
[37] G.M. Jacobsen, R.K. Shoemaker, M.R. DuBois, D.L. DuBois, Organometallics 26 (2007) 4964–4971.
[38] (a) Z.M. Heiden, S. Chen, M.T. Mock, W.G. Dougherty, W.S. Kassel, R. Rousseau, R.M. Bullock, Inorg. Chem. 52 (2013) 4026–4039;
(b) Z.M. Heiden, S. Chen, L.A. Labios, R.M. Bullock, E.D. Walter, E.L. Tyson, M.T. Mock, Organometallics 33 (2014) 1333–1336.
[39] (a) S. Ezzaher, J.-F. Capon, F. Gloaguen, F.Y. Pétillon, P. Schollhammer, J. Talarmin, N. Kervarec, Inorg. Chem. 48 (2009) 2–4;
(b) J.-F. Capon, F. Gloaguen, F.Y. Pétillon, P. Schollhammer, J. Talarmin, Coord. Chem. Rev. 253 (2009) 1476–1494.
[40] (a) J.T. Bays, N. Priyadarshani, M.S. Jeletic, E.B. Hulley, D.L. Miller, J.C. Linehan, W.J. Shaw, ACS Catal. 4 (2014) 3663–3670;
(b) N. Wang, M. Wang, T. Zhang, P. Li, J. Liu, L. Sun, Chem. Commun. (2008) 5800–5802.
[41] T. Katsuki, Chem. Lett. 34 (2005) 1304–1309.
[42] X.Y. Huang, T.M. Bergsten, J.T. Groves, J. Am. Chem. Soc. 137 (2015) 5300–5303.
[43] (a) D.F. Evans, J. Chem. Soc. (1959) 2003–2005;
(b) E.M. Schubert, J. Chem. Educ. 69 (1992) 62.
[44] (a) B.K. Bower, H.G. Tennent, J. Am. Chem. Soc. 94 (1972) 2512–2514;
(b) R.A. Lewis, B.E. Smiles, J.M. Darmon, S.C.E. Stieber, G. Wu, T.W. Hayton, Inorg. Chem. 52 (2013) 8218–8227.
[45] Gaussian 16, Revision A.03, Frisch, M. J. et al. Gaussian, Inc., Wallingford CT, 2016.
[46] A. D. Becke, Phys. Rev. A 38 (1988) 3098–3100; (b) A. D. Becke, A. D. J. Chem. Phys. 98 (1993) 5648–5652.
[47] S. Grimme, J. Antony, S. Ehrlich, H.A. Krieg, J. Chem. Phys. 132 (2010) 154104.
[48] M. Wang, X. Yu, Z. Shi, M. Qian, K. Jin, J. Chen, R. He, J. Organomet. Chem. 645 (2002) 127–133.
[49] (a) H. Zhang, Z. Ouyang, Y. Liu, Q. Zhang, L. Wang, L. Deng, Angew. Chem. Int. Ed. 53 (2014) 8432–8436;
(b) L. Wang, L. Hu, H. Zhang, H. Chen, L. Deng, J. Am. Chem. Soc. 137 (2015) 14196.
[50] C. Ni, J.C. Fettinger, G.J. Long, M. Brynda, P.P. Power, Chem. Commun. (2008) 6045–6047.
[51] P.T. Wolczanski, Organometallics 36 (2017) 622–631.
[52] É. de Brito Sá, L. Rodríguez-Santiago, M. Sodupe, X. Sonlans-Monfort, Organometallics 35 (2016) 3914–3923.
[53] M. Rahm, R. Hoffmann, J. Am. Chem. Soc. 138 (2016) 3731–3744.
[54] R. Hoffmann, S. Alvarez, C. Mealli, A. Falceto, T.J. Cahill 3rd, T. Zeng, G. Manca, Chem. Rev. 116 (2016) 8173–8192.
[55] R.C. Walroth, J.T. Lukens, S.N. MacMillan, K.D. Finkelstein, K.M. Lancaster, J. Am. Chem. Soc. 138 (2016) 1922–1931.
[56] C. Gao, G. Macetti, J. Overgaard, Inorg. Chem. 58 (2019) 2133–2139.
[57] S. Ruccolo, M. Rauch, G. Parkin, Chem. Sci. 8 (2017) 4465–4474.
[58] C.A. Coulson, I. Fischer, Philos. Mag. 40 (1949) 386.
[59] (a) M.D. Hopkins, T.C. Zietlow, V.M. Miskowski, H.B. Gray, J. Am. Chem. Soc. 107 (1985) 510–512;
(b) M.D. Hopkins, H.B. Gray, V.M. Miskowski, Polyhedron 6 (1987) 705–714.
[60] F.A. Cotton, D.G. Nocera, Acc. Chem. Res. 33 (2000) 483–490.
[61] D.C. Rosenfeld, P.T. Wolczanski, K.A. Barakat, C. Buda, T.R. Cundari, J. Am. Chem. Soc. 127 (2005) 8262–8263.
[62] S.P. Heins, W.D. Morris, T.R. Cundari, S.N. MacMillan, E.B. Lobkovsky, N.M. Livezey, P.T. Wolczanski, Organometallics 37 (2018) 3488–3501.